Suppressing tiger stripes:
Taming flow oscillations to improve print quality

S.G. Mallinson, G.D. McBain, G.D. Horrocks, A.J. North, A.P. O'Mahony, P.J. Reichl,

S.J. Myers, J.J. Miller, B. Powell, J. Hess, D.R. Secker, P.C. Palma

Memjet, Macquarie Park NSW 2113, Australia

Abstract

The problem of tiger striping is described: oscillations of the print-jet cause re-deposition of small aerosols far from their intended location on the print-media. Experimental and numerical studies of the problem have shown the main factors and possible mitigation strategies for this print quality artefact.

Introduction

Single-pass inkjet printers deposit a page-wide swath of droplets onto media which moves parallel to the print-face, in contrast with scanning printers, which build up the image by printing small parts of the image in sequence. In single-pass inkjet printers, the interaction between the jet induced by droplet ejection and the cross-flow generated by media motion can cause unsteadiness of the vortices in the printhead-to-media gap. This unsteadiness causes low Stokes number particles to be carried by the flow and redeposited onto the media in such a way as to produce a visible print artefact called 'tiger striping', 'sand duning' or 'wood graining' [1], see Figure 1.

Figure 1. Print sample showing 'tiger striping'.

Here, we discuss the important factors in the occurrence of tiger striping, as determined by experimental testing and numerical modelling. We then introduce two methods for mitigating against this phenomenon.

Theory
Droplet and Printing Characteristics
The majority of this work was conducted with the first generation of Memjet printheads. These ejected main droplets with volume approximately 1.5 pL travelling at approximately 10 m s^{-1}. The inks are aqueous with a density very close to that of water. The test environment was a laboratory with temperature 25 °C. Smaller satellite droplets are also ejected, typically one or more per main droplet, with volumes in the range 5-200 fL. The media is located approximately 1-2 mm from the print-face, and it moves relative to the printhead at speeds up to approximately 75 A4 pages-per-minutes (ppm), or 0.37 m s^{-1}.

Non-Dimensional Parameters
The motion of droplets in a flowing stream can be characterized by the Stokes number, S, which is the ratio of the characteristic particle time [2]:

$$t_p = \frac{\rho_p d_p^2}{18\mu_\infty} \tag{1}$$

to the characteristic flow time:

$$t_f = \frac{d_f}{|U_f - U_p|} \tag{2}$$

Thus:

$$S = \frac{t_p}{t_f} = \frac{\rho_p d_p^2 |U_f - U_p|}{18\mu_\infty d_f} \tag{3}$$
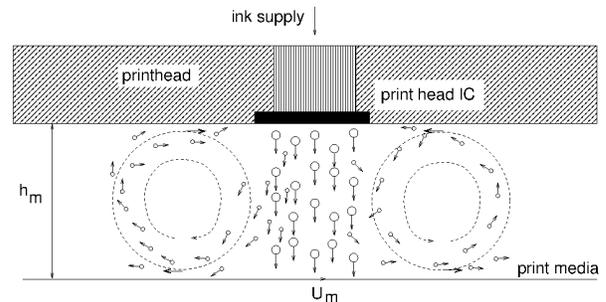
Figure 2. Schematic of the print-zone (not to scale), wherein the printhead IC (PHIC) ejects droplets from several locations onto media located h_m away from the PHIC and which moves at a speed U_m. The flow induced by the large droplets causes counter-rotating vortices to be situated either side of the PHIC; these vortices trap smaller particles which can then be re-deposited.

Here, ρ = density, d = size (or diameter), μ = viscosity, U = velocity, and the subscripts 'p', 'f' and '∞' refer to particle, flow and ambient values, respectively. For large values of the S, the particles are not affected by the flow, whilst for small S, the particles are carried by the flow. For flow in the printhead-to-paper gap, shown schematically in Figure 2, the flow velocity and length-scale are the media speed, $U_f \approx U_m$, and printhead-to-media gap height, $d_f \approx h_m$. For the main droplets, $S \approx 10$, suggesting that they remain unaffected by the cross flow due to the media motion. For the satellites, the range is $0.1 \leq S \leq 1$, meaning that they are carried along by the induced flow.

As the main droplets travel through the print gap, they slow due to drag, and eventually, their instantaneous Stokes number will be of order 1 or less and so they too will become carried along by the flow. The distance from the printhead at which this occurs is

usually called the range, and it can be estimated as the product of the droplet relaxation time, equation (1) and the initial velocity. For Memjet printers, the range is approximately 6 mm. The useful range is, however, limited by the fact that above a certain media height, the print jet becomes unstable and tiger striping is observed in prints. This limits the range of media thickness that can be accommodated within a given printing system: a printer which is supposed to print on envelopes (thickness > 5 mm) will require a large print gap, say 6 mm, to keep the media height under the critical value where tiger striping becomes objectionable; for the same print gap, standard papers with weights in the range 80 – 300 grams per square meter (gsm) which have a thickness of approximately 0.1 – 0.35 mm, will then have a media height which approaches the range, and so tiger stripes will be an issue for those media.

The main droplet Reynolds number is approximately 25, whilst the satellite droplet Reynolds number range is approximately 3-12. The Reynolds number of the gap is approximately 260. These values are small enough that turbulence is not present and so a laminar model should suffice.

Method

Experimental Testing
Experimental tests were conducted on two different test printing systems.

The first involved a single chip mounted on top of a reservoir of ink, with the media held fixed whilst the print chip moved over the surface. This system was used for print testing. Printing tests involved forcing a fraction (up to 100%) of the actuators in a single or multiple (up to five) colour plane(s) to fire with a frequency of operation from 2 to 11 kHz. A glossy print media was selected as this highlights any print density modulation. This phase of experimental testing revealed that the main factors modulating the occurrence of tiger striping are: media height, paper speed, droplet size and printing density. All other things being equal, it is desirable to have a media height as large as possible to provide flexibility in the acceptable media types.

The second was an eleven chip printhead (A4 width) mounted in a printer without covers, to permit access for visualization. In this instance, the media moved under the printhead. Flow visualization was performed using a light sheet formed by passing a collimated HeNe laser beam through a cylindrical lens. The sheet was aligned with the droplet firing direction, with the droplets themselves providing the scattering. The images were captured using an AVT Pike 302b CCD camera.

Numerical Simulations
Transient solutions of the Navier-Stokes equations using Lagrangian treatment of the droplets were performed using ANSYS-Fluent-15. The droplets were two-way coupled to the flow, although it was found that the smaller droplets could be modelled without coupling without any change to the results. The print-zone geometry was created in SolidWorks and exported for defeaturing using ANSYS-DesignModeler. The spatial derivatives are handled using least-squares cell-based values, the pressure is solved using the PRESTO! (PREssure Staggering Option, similar to the method outlined by Patankar [6]), whilst the momentum is solved via a second-order upwind scheme. The time stepping was second order implicit.

The particles are given an initial velocity normal to the print-face. Gravity and drag forces are computed at each time step, and their motion is tracked in time. The drag law for the particles was taken as one for spherical particles described in [5].

The simulation results were post-processed to produce numerical prints. Computational fluid dynamics simulations of ejection across the page gap lead to large sets of data in terms of dot placement which require synthesis. A natural measure to look for is the optical density and its spatial variation. Here we developed numerical techniques for constructing optical density field from dot placement vectors. If drops fall reasonably regularly on the page, it is possible to relate the optical density and the dot placement vector field. This approach works by treating the discrete data as samples of an underlying fictitious smooth vector field, which can then be subject to the techniques of vector calculus and analytical continuum mechanics.

Consider a single collinear row of nozzles firing simultaneously and periodically such that ideally the jth actuation of the ith nozzle will put a dot at (X_i, Y_j), where ΔX_i ($\equiv X_{i+1} - X_i$) and ΔY_j are constant, i.e. independent of i and j, so we can drop the subscripts. Actually the $(i, j)^{\text{th}}$ dot lands at $(x_{ij}, y_{ij}) = (X_i + u_{ij}, Y_j + v_{ij})$ due to its misdirection (u_{ij}, v_{ij}).

That is, one dot lands not on X but on $X + u$ and that fired simultaneously from the neighbouring nozzle not on $X + \Delta X$ but on $X + \Delta X + u + \Delta u$. Thus the x-component of their separation is not ΔX but $\Delta X + \Delta u$. Similarly the y-component of the separation between successive dots from the same nozzle is $\Delta Y + \Delta v$. Thus the area of the rectangular cell of dots is not $A \equiv \Delta X \, \Delta Y$ but

$$(\Delta Y + \Delta v)\,(\Delta X + \Delta u) = \Delta Y \, \Delta X + \Delta Y \, \Delta u + \Delta X \, \Delta v + \Delta v \, \Delta u$$
$$= \Delta Y \Delta X \, (1 + \Delta u \,/\, \Delta X + \Delta v \,/\, \Delta Y) + \Delta u \, \Delta v$$
$$\sim A \, (1 + \Theta) + \text{higher order terms} \qquad (4)$$

where

$$\Theta \equiv \partial u \,/\, \partial x + \partial v \,/\, \partial y \qquad (5)$$

is the divergence of the dot displacement field.

The ideal rectangular grid has one dot per cell of area $\Delta X \, \Delta Y$, but the actual cell is distorted to have an area approximately $1 + \Theta$ times that. Since this cell still only contains one dot, the areal density of dots is divided by a factor $1 + \Theta$.

This is exactly analogous to the formula for the change in volume of a small portion of a body subject to strain [3] which says that the divergence of the displacement is equal to the 'increment of volume per unit volume or the "cubical dilatation", often called the "dilatation"'.

To within the limits of this linear approximation, we can use the Maclaurin series $1 \,/\, (1 + \Theta) \sim 1 - \Theta + \mathrm{O}\,(\Theta^2)$, and so take the optical density field as proportional to $1 - \Theta$; i.e. the divergence is the relative defect of optical density.

In graphing this relative optical density field, $1 - \Theta$, the value should be associated with the displaced point (x_{ij}, y_{ij}) rather than the ideal point (X_i, Y_j), in such cases where the displacement is large enough that this makes a difference. Here we explicitly have in mind cases in which the displacement is large though the gradients of displacement are small enough for the displacement to be smooth from nozzle to nozzle and actuation to actuation. The assumption is $\|(\Delta u, \Delta v)\| \ll \|(\Delta X, \Delta Y)\|$.

An experimental print is show in Figure 3, constructed from the misplacement of 6 µm diameter droplets. The larger droplets pass almost straight through the printhead-to-media gap. This suggests that in this instance, the tiger striping phenomenon is due to misplacement of the smaller satellite droplets.
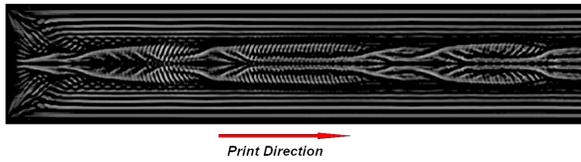
Figure 3. Numerical print.
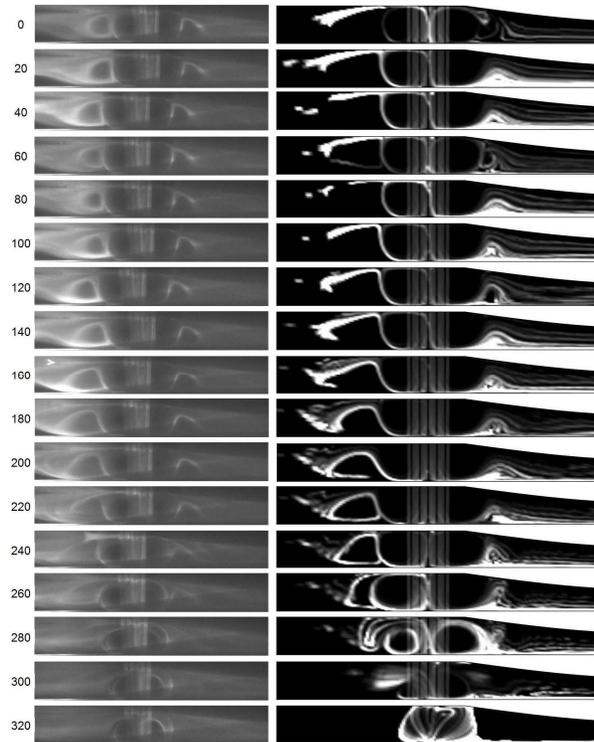
Figure 4. Comparison of experimental (left) and numerical (right) droplet concentration. The numbers at the left refer to the number of actuators from the centre of the printing region. Flow is from left-to-right.
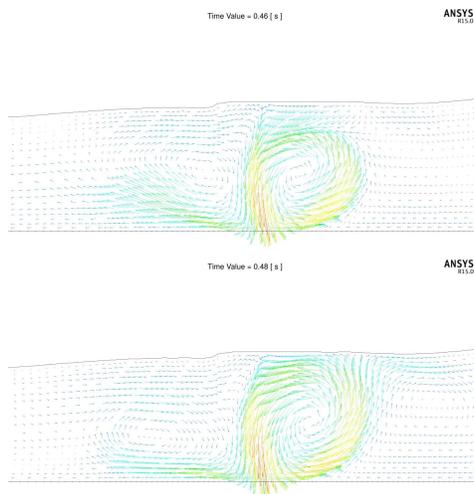
Figure 5. Instantaneous vector fields near the printhead. Paper motion is from right–to-left.

Results
Baseline Flow

The simulation predictions were validated by comparing against experimental flow visualization data at a number of cross-

printhead locations. The print test consisted of repeated cycles of firing of a single colour plane followed by firing all colour planes. In each instance, a swath of 630 nozzles per colour plane were fired with a 10 nozzle gap in the centre (that is, one chip width). The media gap height was set as 0.8 mm, the firing frequency was 11 kHz and the paper speed was set at 0.175 m s^{-1}. The numerical predictions were post-processed to determine the particle concentration, these field values were re-scaled to the range [0, 1] and contours of concentration plotted in the planes of interest. The comparison is presented in Figure 4.
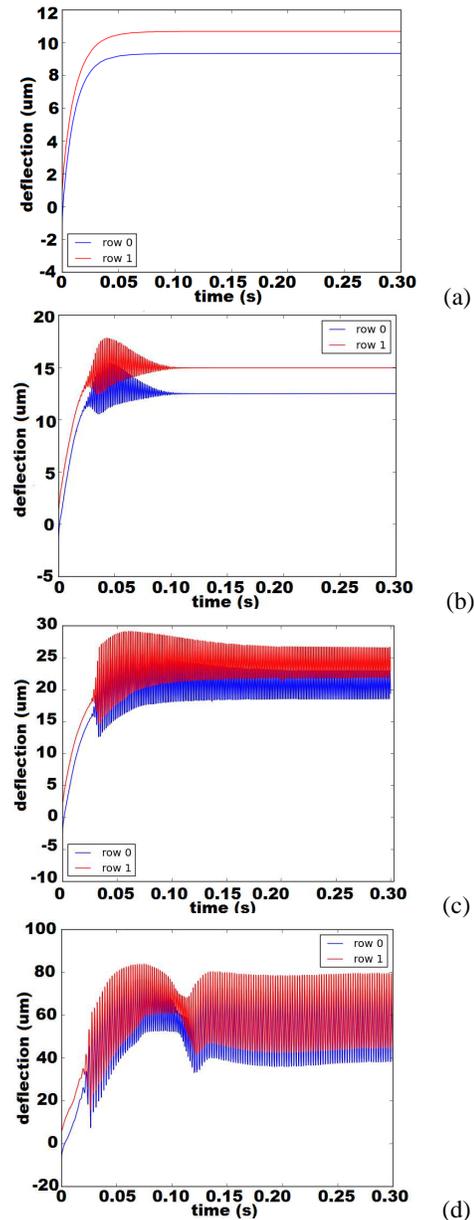
Figure 6. Deflection of main droplets as a function of time for two rows of a single colour plane. (a) $h_m = 1$ mm; (b) $h_m = 1.7$ mm; (c) $h_m = 2$ mm; (d) $h_m = 3$ mm.

The velocity vectors on the centre-plane are shown in Figure 5 for two instants spaced shortly apart in time. The paper motion is from right-to-left. The flow field is seen to change dramatically over the duration displayed, with the vortex downstream of the high speed jet growing, whilst the vortex just upstream, near the print-face, shrinks. We can also track the droplet y-misplacement (that is, in the same direction as the paper motion) as a function of time

(Figure 6) which shows highly unstable behaviour. Four plots are shown for different values of media height, highlighting the impact of this design parameter on the unsteadiness of the flow. For these plots, the misplacement is averaged over all of the actuators simulated in the two rows.

Mitigation Strategies
The flow-field resulting from the interaction of the jet induced by the droplets and the shear flow induced by the paper motion appears to be nearly symmetrical about the centre of the printhead. This suggested a strategy of symmetry breaking to reduce the impact of flow unsteadiness.

First, a pressure difference was applied between the upstream and downstream ends of the domain. This proved quite effective as evidenced by the absence of oscillation in the droplet deflection shown in Figure 7 for the case of pressure differences = +/- 1 Pa.

(a)

(b)
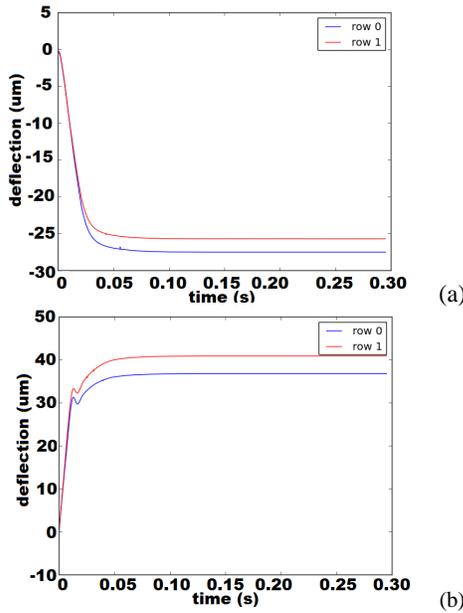
Figure 7. Deflection of main droplets with pressure difference applied between upstream and downstream ends of simulation domain, $h_m = 2$ mm. (a) pressure difference = 1 Pa; (b) pressure difference = -1 Pa.
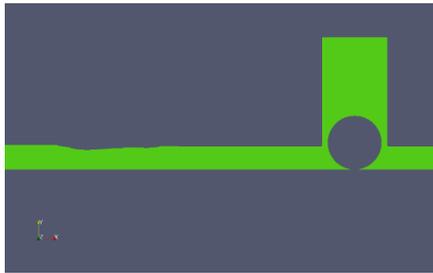
Figure 8. Print-zone with upstream roller, paper moving right-to-left.

Next, whilst considering system integration, it was realized [4] that a paper handling component, a roller upstream of the print-zone (see Figure 8), could provide a pressure difference. The roller induces a small flow caused by shear with the surrounding air as it rotates. The effect is similar to applying a smaller pressure difference than was used in the earlier simulations (Figure 7). The predicted main droplet deflection shown in Figure 9, together with

the numerical prints shown in Figure 10, suggests that use of an upstream roller is an effective strategy to mitigate against flow unsteadiness and to tame tiger striping.
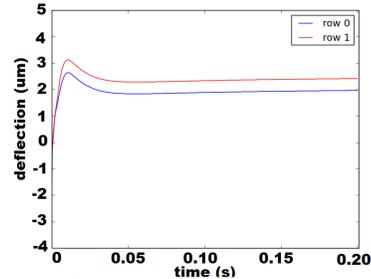
Figure 9. Droplet deflection with roller in place, $h_m = 2$ mm.
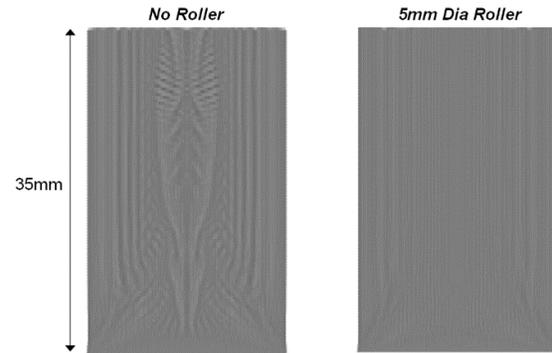
Figure 10. Comparison of numerical prints with and without roller.

Conclusions
Flow in the print zone of a single pass printing simulation has been characterized experimentally using laser light sheet visualization and print testing. Numerical simulations using Lagrangian treatment of the ejected droplets compare well with both data sets. For sufficiently high printhead-to-media gap heights, the flow becomes unsteady which results in patterns on the print which are reminiscent of tiger stripes. The numerical model was used to assess two different mitigation strategies to suppress tiger stripes: application of a pressure difference between the upstream and downstream ends of the print-zone, and inclusion of a roller which partially blocks the flow. Both strategies were observed to dramatically reduce the incidence of tiger striping.

References
[1] Barnett, D. & McDonald, M., Evaluation and Reduction of Elevated Height Printing Defects, *In: Proc. Int. Conf. on Digital Printing Technologies*, 2014, pp. 38-43(6)
[2] Crowe, C.T., Troutt, T.R. & Chung, J.N., Particle Interactions with Vortices, In Green, S.T. (ed.) *Fluid Vortices*, Chap. 19, Kluwer Press, 1995.
[3] Love, A. E. H., *A Treatise on the Mathematical Theory of Elasticity*, Dover, 1944.
[4] Miller, J.J., Reichl, P.J., Myers, S.J., Horrocks, G.D., O'Mahony, A.P. & Mallinson, S.G., Printer with Reduced Vortex Oscillation in Print Gap, *US Patent* 8382243, 2013.
[5] Morsi, S. A. & Alexander, A. J., An Investigation of Particle Trajectories in Two-Phase Flow Systems, *J. Fluid Mech.*, **55**, 1972, 193-208.
[6] Patankar, S. V., *Numerical Heat Transfer and Fluid Flow*, Hemisphere, 1980.